

# Hop-Count Based Self-Supervised Anomaly Detection on Attributed Networks

Tianjin Huang<sup>\*</sup>, Yulong Pei<sup>\*</sup>, Vlado Menkovski, Mykola Pechenizkiy

**Abstract**—A number of approaches for anomaly detection on attributed networks have been proposed. However, most of them suffer from two major limitations: (1) they rely on unsupervised approaches which are intrinsically less effective due to the lack of supervisory signals of what information is relevant for capturing anomalies, and (2) they rely only on using local, e.g., one- or two-hop away node neighbourhood information, but ignore the more global context. Since anomalous nodes differ from normal nodes in structures and attributes, it is intuitive that the distance between anomalous nodes and their neighbors should be larger than that between normal nodes and their (also normal) neighbors if we remove the edges connecting anomalous and normal nodes. Thus, estimating hop counts based on both global and local contextual information can help us to construct an anomaly indicator. Following this intuition, we propose a hop-count based model (HCM) that achieves that. Our approach includes two important learning components: (1) self-supervised learning task of predicting shortest path length between a pair of nodes, and (2) Bayesian learning to train HCM for capturing uncertainty in learned parameters and avoiding overfitting. Extensive experiments on real-world attributed networks demonstrate that HCM consistently outperform state-of-the-art approaches.

**Index Terms**—Anomaly detection, Self-supervised learning, Graph convolutional networks, global and local contextual information.

## 1 INTRODUCTION

ATTRIBUTED networks are ubiquitous in a variety of real-world applications. Attributed networks can be utilized to represent data from different domains. For example, in a social network, each node can represent a user, an edge denotes the friend relation between users, and user profiles are the attributes to describe users. A citation network consists of papers as the nodes, citation relations as the edges, and words in paper abstracts can be the attributes of papers. Unlike plain networks where only structural information exists, attributed networks also contain rich features to provide more details to describe (elements of) networks. Due to the ubiquity of attributed networks, various tasks on attributed networks have been widely studied such as community detection [1], [2], link prediction [3], [4], network embedding [5], [6] etc.

Among these tasks on attributed networks, anomaly detection is perhaps one of the most important ones in the current analytics tasks – it can shed light on a wide range of real-world applications such as fraud detection in finance and spammers discovery in social media.

Figure 1 shows a toy example of anomalies on an attributed network where nodes 10 and 11 are anomalies. Unlike in anomaly detection on plain networks, detecting anomalies on attributed networks should rely on two sources of information: (1) the structural patterns of how nodes interconnect or interact with each other, which are reflected by the topological structures, (2) the distributions of nodal features. Therefore, it is more challenging to detect

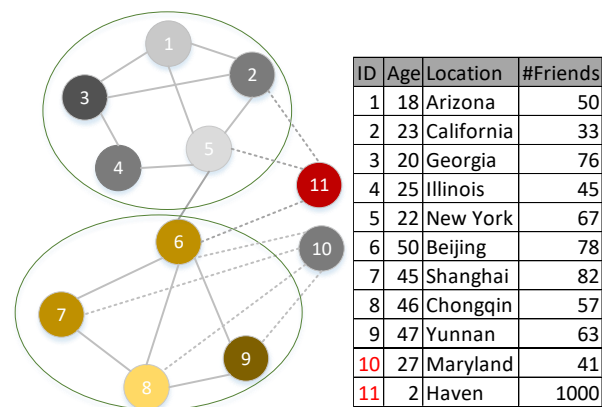


Fig. 1: A toy example for illustrating anomalies on attributed networks.

anomalies on attributed networks.

To solve this challenging problem, various supervised and unsupervised approaches have been proposed recently. Unsupervised anomaly detection methods are preferable in practice because of the prohibitive cost for accessing the ground-truth anomalies [7]. Hence, in this study, we focus on unsupervised fashion to detect anomalies in the sense that we do not require access to ground truth anomalies in the training data to induce a model. Previous studies can be categorized into three types: community analysis, subspace selection, and residual analysis. Community analysis methods [8] detect anomalies by identifying current node’s abnormality with other nodes within the same community. Subspace selection approaches [9] learn a subspace for features and then discover anomalies in the learned subspace.

- T. Huang is with Eindhoven University of Technology, 5600MB Eindhoven, the Netherlands.  
E-mail: t.huang@tue.nl
- Y. Pei, V. Menkovski and M. Pechenizkiy are with Eindhoven University of Technology, 5600 MB Eindhoven, the Netherlands.

\*. Equal contribution

Residual analysis methods [10], [11] explicitly model the residual information by reconstructing the input attributed network based on matrix factorization. With the popularity of deep learning techniques, methods use deep neural networks such as graph convolutional networks (GCN) and network embedding to capture the nonlinearity of networks and detect anomalies have been proposed [7], [12], [13].

Intrinsically, unsupervised learning approached demonstrate worse performance than supervised learning approaches (when they are applicable) due to the lack of supervisory signals. Recently, various self-supervised techniques have been proposed to learn a better feature representation via designing supervisory signals directly from input data. It has been shown e.g. in computer vision domain that self-supervised learning can improve model’s robustness and uncertainty estimation, including robustness to adversarial examples, label corruption, detecting out-of-distribution on difficulty, near-distribution outliers etc [14].

In this paper, we employ the idea of self-supervised learning by forcing the prediction of shortest path length between pairs of nodes (denoted as hop counts for convenience) to detect anomalies on attributed networks. This idea allows to address another limitation of existing approaches that utilize only local context of nodes to detect anomalous nodes while neglecting the global context information that provides a complementary view of the network structure patterns including anomalous structures. It has been shown that the global context of node is helpful to learn node representation that can finely characterize the similarity and differentiation between nodes [15]. Global structures, which can be modeled by  $k$ -step relations ( $k > 2$ ) [16], roles and positions [17], and high-order motifs [18], have been found important in describing the structural patterns of graph data [19]. Therefore, it is reasonable to assume that effectively anomaly detection methods should consider local and global contextual information.

### 1.1 Problem Settings

Following the commonly used notations, we use bold uppercase characters for matrices, e.g.,  $\mathbf{X}$ , bold lowercase characters for vectors, e.g.,  $\mathbf{b}$ , and normal lowercase characters for scalars, e.g.,  $c$ . The  $i^{\text{th}}$  row of a matrix  $\mathbf{X}$  is denoted by  $\mathbf{X}_{i,:}$  and  $(i, j)^{\text{th}}$  element of matrix  $\mathbf{X}$  is denoted as  $\mathbf{X}_{i,j}$ . The Frobenius and  $L_2$  norm of a matrix are represented as  $\|\cdot\|_F$  and  $\|\cdot\|_2$  respectively. The number of elements of a set is denoted by  $|\cdot|$ .

**Definition 1. Attributed Networks.** An attributed network  $\mathcal{G} = \{V, E, \mathbf{X}\}$  consists of: (1) a set of nodes  $V = \{v_1, v_2, \dots, v_n\}$ , where  $|V| = n$  is the number of nodes; (2) a set of edges  $E$ , where  $|E| = m$  is the number of edges; and (3) the node attribute matrix  $\mathbf{X} \in \mathbb{R}^{n \times d}$ , the  $i^{\text{th}}$  row vector  $\mathbf{X}_{i,:} \in \mathbb{R}^d$ ,  $i = 1, \dots, n$  is the attribute of node  $v_i$ .

The topological structure of attributed network  $\mathcal{G}$  can be represented by an adjacency matrix  $\mathbf{A}$ , where  $\mathbf{A}_{i,j} = 1$  if there is an edge between node  $v_i$  and node  $v_j$ . Otherwise,  $\mathbf{A}_{i,j} = 0$ . We focus on the undirected networks in this study and it is trivial to extend it to directed networks. The attribute of  $\mathcal{G}$  can be represented by an attribute matrix  $\mathbf{X}$ . Thus, the attributed network can be represented as

$\mathcal{G} = \{\mathbf{A}, \mathbf{X}\}$ . With these notations and definitions, same to previous studies [7], [10], [11], [13], we formulate the task of anomaly detection on attributed networks:

#### Problem 1. Anomaly Detection on Attributed Networks.

Given an attributed network  $\mathcal{G} = \{\mathbf{A}, \mathbf{X}\}$ , which is represented by the adjacency matrix  $\mathbf{A}$  and attribute matrix  $\mathbf{X}$ , the task of anomaly detection is to find a set of nodes that are rare and differ singularly from the majority reference nodes of the input network.

### 1.2 Our HCM approach in a nutshell.

We use hop count prediction as a self-supervised learning task to capture local and global contextual information for node representation. We use GCN to learn node representations for refining the graph. Then the learned node representation is used to predict hop counts for arbitrary node pairs. We design two anomaly scores based on the intuition that the true hop-count between anomalous nodes and their neighbors shall be larger than that between normal nodes and their neighbors, e.g. in our toy example in Figure 1, the hop counts between node 10 and their neighbors should be larger than 1 since node 10 is from the community with gray colors.

We adopt Bayesian learning to train our HCM model because Bayesian methods are appealing in their ability to capture uncertainty in learned parameters and avoid overfitting [20]. Specifically, we exploit Stochastic Gradient Langevin Dynamics (SGLD) [20] to optimize our model and conduct Bayesian inference.

### 1.3 Summary of the contributions

The contributions of this paper are summarized as follows:

- We are the first (to the best of our knowledge) to employ self-supervised learning ideas in the graph anomaly detection domain and to make use of both global and local contextual information of nodes, i.e., hop counts, to detect anomalies on attributed networks.
- With the help of the self-supervised learning technique, we propose our HCM model to learn node representations capturing local and global contextual information of nodes. And based on the HCM model, we design two anomaly scores to detect anomalies. Experimental results demonstrate the effectiveness of our approach.
- We exploit SGLD to optimize HCM model for capturing uncertainty in learned parameters and avoid overfitting. We experimentally demonstrate that our model optimized by SGLD performs better than SGD in anomaly detection. Besides, SGLD achieves a steadier behaviour during the training process.

### 1.4 Paper outline

The rest of this paper is organized as follows. Section 2 introduces the proposed hop-count-based model. We present the overall framework, model training and model inference approaches as well as complexity analysis of the model. In Section 3 we explain how we empirically evaluated the proposed method on anomaly detection task using various real-world networks and compared its performance against

several state-of-the-art anomaly detection techniques. Then we discuss the obtained results. Section 4 briefly summarises related works on anomaly detection on attributed networks and self-supervised learning. Finally we conclude in Section 5.

## 2 HOP-COUNT BASED MODEL

In this section we first present a detailed description for our proposed HCM model. Then the SGLD optimization strategy will be introduced. Finally, we discuss the anomaly scores based on different strategies.

### 2.1 Model Framework

In this section, we introduce the framework of our proposed HCM model in detail. HCM model is based on self-supervised task that is designed by some innate characteristics of the data. Recently, several self-supervised tasks have been proposed for graph data. For example, node clustering task where a clustering operation will be used to provide pseudo labels; Graph partition task where graph partitioning will provide pseudo labels [21]; PairDistance task where hop counts of node pairs are used as label [22]; PairwiseAttrSim where the similarities of node pairs are taken as label [22]. Here we adopt PairDistance as our self-supervised task. There are three reasons accounting for using PairDistance as our self-supervised task: 1) It is cheap to get the true label during the training process; 2) The hop counts capture both global and local information of a network; 3) hop counts can be utilized to directly construct anomaly scores of nodes. Our HCM model is composed of three components (Fig. 2): Preprocess components, Graph Convolutional network (GCN) and Multilayer perception (MLP). Preprocess is to generate labels during training process; GCN is to learn the representation of the attributes networks; MLP is the classifier to predict hop counts for node pairs.

#### 2.1.1 Preprocess

There are two operations in Preprocess component. The first is to drop edges with small similarities in adjacency matrix. The second is to generate labels, namely the hop counts of all node pairs.

**Drop Edges** Considering that the anomalies on the attribute network could potentially perturb links, we remove some edges in adjacency matrix before utilizing it to generate labels. Specifically, we remove the potential perturbed links according to the similarities of node pairs. [23] has been demonstrated that removing links with small similarities can effectively purify perturbed links, especially for adversarial perturbed links. Similar to [23], for binary features, we adopt the Jaccard similarity to measure the similarities:

$$S_{Jar}(i, j) = \frac{|\mathbf{X}_{i,:} \cap \mathbf{X}_{j,:}|}{|\mathbf{X}_{i,:} \cup \mathbf{X}_{j,:}|}. \quad (1)$$

For continuous features, we adopt the Cosine similarity to measure the similarities:

$$S_{Sin}(i, j) = \frac{\mathbf{X}_{i,:}^T \mathbf{X}_{j,:}}{\|\mathbf{X}_{i,:}\|_2 \|\mathbf{X}_{j,:}\|_2}. \quad (2)$$

We use the hyper-parameter drop ratio  $R$  to control the percentage of links that will be removed.

**Generate Labels** After dropping some edges, the modified adjacency matrix will be used to generate labels. Specifically, we firstly utilize Dijkstra search algorithm to calculate the hop counts for all node pairs:  $Y_{hop}^1 = \{(v_m, v_n) | \text{hop}(v_m, v_n) = 1, v_m, v_n \in V\}$ ,  $Y_{hop}^2 = \{(v_m, v_n) | \text{hop}(v_m, v_n) = 2, v_m, v_n \in V\}$ ,  $Y_{hop}^3 = \{(v_m, v_n) | \text{hop}(v_m, v_n) = 3, v_m, v_n \in V\}$ ...,  $Y_{hop}^i = \{(v_m, v_n) | \text{hop}(v_m, v_n) = i, v_m, v_n \in V\}$ , where  $\text{hop}(v_m, v_n)$  denotes the hop counts between node  $v_m$  and  $v_n$ . Then these hop counts will be grouped into  $C$  classes:  $\text{hop}(v_m, v_n) = 1, \text{hop}(v_m, v_n) = 2, \dots, \text{hop}(v_m, v_n) \geq C$ . Besides, Considering that the  $|Y_{hop}^i|$  are different for each set  $Y_{hop}^i$ , which will lead to imbalanced training set. In order to avoid the bias induced by imbalanced training set, we sampling a same amount of node pairs from each set  $Y_{hop}^i$  during the training, the amount of node pairs is decided by the smallest  $|Y_{hop}^i| \cdot S$  where  $S$  is sampling ratio.

#### 2.1.2 GCN

GCN learns node representations by passing and aggregating messages between neighboring nodes. Different types of GCN have been proposed recently [24], [25], and we focus on one of the most widely used versions proposed in [24]. Formally, a GCN is defined as

$$\mathbf{h}_i^{(l+1)} = f\left(\sum_{j \in Ne(i)} \frac{1}{\sqrt{\tilde{\mathbf{D}}_{i,i} \tilde{\mathbf{D}}_{j,j}}} \mathbf{h}_j^{(l)} \mathbf{W}^{(l)}\right), \quad (3)$$

where  $\mathbf{h}_i^{(l)}$  is the latent representation of node  $v_i$  in layer  $l$ ,  $Ne(i)$  is the set of neighbors of node  $v_i$ , and  $\mathbf{W}^{(l)}$  is the layer-specific trainable weight matrix.  $f(\cdot)$  is a non-linear activation function and we select ReLU as the activation function following previous studies [24] (written as  $f_{ReLU}(\cdot)$  below).  $\tilde{\mathbf{D}}$  is the diagonal degree matrix of  $\tilde{\mathbf{A}}$  defined as  $\tilde{\mathbf{D}}_{i,i} = \sum_j \tilde{\mathbf{A}}_{i,j}$  where  $\tilde{\mathbf{A}} = \mathbf{A} + \mathbf{I}$  is the adjacency matrix of the input attributed network  $\mathbf{G}$  with self connections  $\mathbf{I}$ . Equivalently, we can rewrite GCN in a matrix form:

$$\mathbf{H}^{(l+1)} = f_{ReLU}\left(\tilde{\mathbf{D}}^{-\frac{1}{2}} \tilde{\mathbf{A}} \tilde{\mathbf{D}}^{-\frac{1}{2}} \mathbf{H}^{(l)} \mathbf{W}^{(l)}\right). \quad (4)$$

For the first layer,  $\mathbf{H}^{(0)} = \mathbf{X}$  is the attribute matrix of the input network. Therefore, we have

$$\mathbf{H}^{(1)} = f_{ReLU}\left(\tilde{\mathbf{A}} \mathbf{X} \mathbf{W}^{(0)}\right). \quad (5)$$

In this paper, we denote the representation learned by the GCN as  $\mathbf{Z}$ .

#### 2.1.3 MLP

The target of MLP component is to construct hop counts prediction task. MLP is composed of multiple fully connected layers. During training phase, CrossEntropy loss is used to construct supervisory signals. During inference, it predicts hop counts for any arbitrary node pair representations. Given any node pairs  $\mathbf{Z}_{m,:}$  and  $\mathbf{Z}_{n,:}$ , it can be formally expressed as following:

$$\mathbf{z}_d = |\mathbf{Z}_{m,:} - \mathbf{Z}_{n,:}| \quad (6)$$

$$F_{mlp}(v_m, v_n) = f_{ReLU}^k(\mathbf{z}_d \cdot \mathbf{W}), \quad (7)$$

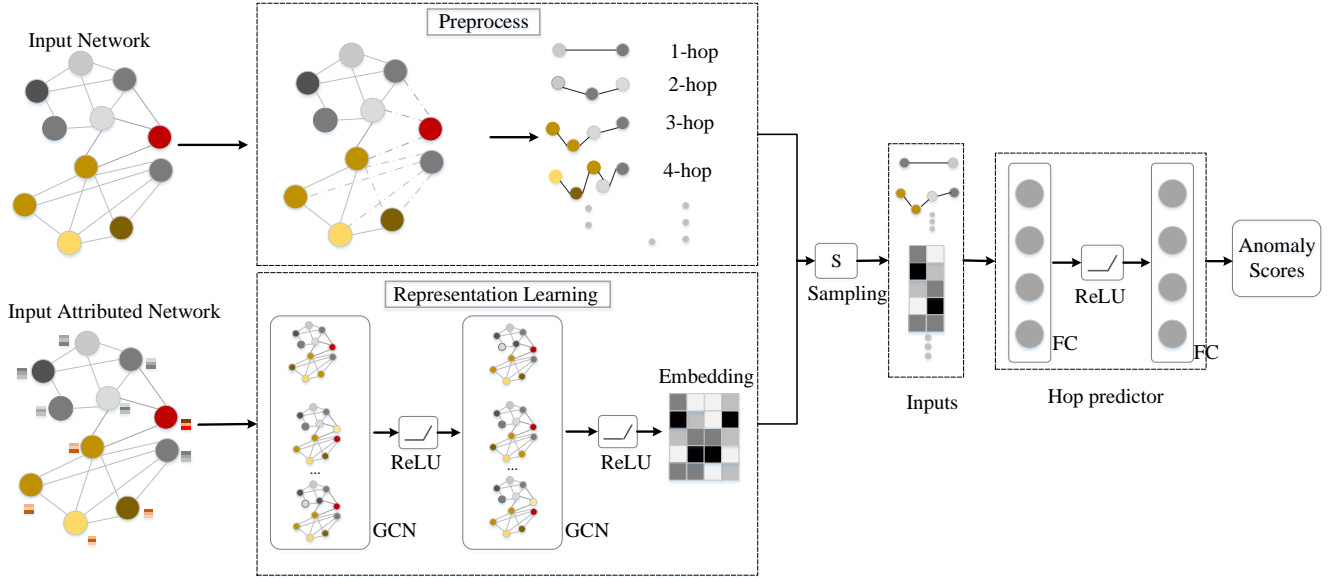


Fig. 2: The framework of our proposed HCM model. The dotted lines in Preprocess component denote the dropped edges.

where  $F_{mlp}(v_m, v_n)$  is the hop counts prediction of node  $v_m$  and  $v_n$ ,  $f_{ReLU}^k$  is  $k$  fully connected layers,  $\mathbf{W}$  is total trainable weight matrix of MLP and  $|\cdot|$  is absolute function. The reason for using absolute function is based on the consideration that the hop counts from node  $Z_{m,:}$  to  $Z_{n,:}$  and from node  $Z_{n,:}$  to  $Z_{m,:}$  are the same on undirected networks. For directed networks, absolute function can be removed.

For the convenience of formulation, we denote the whole model as follows:

$$F_{\mathbf{w}}(\mathbf{X}, \mathbf{A}) = F_{mlp}(v_m, v_n) \circ H^l, \quad (8)$$

where  $\mathbf{w} \in \Omega$  are the parameters of the HCM model and it contains parameters from GCN and MLP components.

### 2.1.4 The Self-supervised Learning Loss

As described above, we adopt PairDistance as the self-supervised task. PairDistance task is to predict hop counts for any given node pairs. And it can be formulate as a multi-class classification problem. Therefore, we formulate the self-supervised learning loss as follows:

$$\mathcal{L}_{self}(\mathbf{w}, \mathbf{A}, \mathbf{X}) = \frac{1}{|\mathcal{S}|} \sum_{(v_m, v_j) \in \mathcal{S}} L(F_{mlp}(v_m, v_n), hop(v_m, v_n)), \quad (9)$$

where  $\mathcal{S}$  is a set of randomly sampled node Pairs and  $L(\cdot)$  is the CrossEntropy loss.

## 2.2 Model Training

The Bayesian framework suggests that the parameters of a model are random variables instead of determined. Therefore, it is crucial to estimate the distribution of model parameters. According to Bayes' theorem, the posterior distribution of the parameters can be defined as follows:

$$p(\mathbf{w}|\mathbf{X}, \mathbf{A}, \mathbf{Y}_{hop}) = \frac{p(\mathbf{Y}_{hop}|\mathbf{X}, \mathbf{A}, \mathbf{w})p(\mathbf{w})}{p(\mathbf{Y}_{hop}|\mathbf{X}, \mathbf{A})}, \quad (10)$$

where  $p(\mathbf{w})$  is a prior distribution for the model's parameters  $\mathbf{w}$ .

According to Eq.(10), there are two different approaches to do the inference:(1) Maximum posterior probability (MAP) estimation finds the mode of the posterior distribution. (2) Bayesian inference computes the posterior distribution itself. Considering that the MAP-estimation can not capture the model's uncertainty, we choose the second approach as our solution. The Bayesian inference of outputs is given as followings:

$$p(y_{hop}^*|x^*, \mathbf{X}, \mathbf{A}, \mathbf{Y}_{hop}) = \int_{\Omega} p(y^*|x^*, \mathbf{w})p(\mathbf{w}|\mathbf{X}, \mathbf{A}, \mathbf{Y}_{hop})d\mathbf{w}, \quad (11)$$

Due to the integration, it is impossible to achieve the prediction by computing the Eq.(11) directly. Fortunately, Stochastic gradient Langevin dynamics (SGLD) [20] provides a general framework to solve Eq. (11). The SGLD update is defined as follows:

$$\delta_{\mathbf{w}_t} = \frac{\epsilon_t}{2} (\nabla_{\mathbf{w}_t} \log p(y_{hop}|\mathbf{w}_t) + \nabla_{\mathbf{w}_t} \log p(\mathbf{w}_t)) + \eta_t \quad (12)$$

$$\eta_t \in N(0, \epsilon) \quad (13)$$

$$\mathbf{w}_{t+1} = \mathbf{w}_t - \delta_{\mathbf{w}_t}, \quad (14)$$

where  $\epsilon_t$  is the step size. The log prior term will be implemented as weight decay. [20] has shown that under suitable conditions, e.g.,  $\sum \epsilon_t = \infty$  and  $\sum \epsilon_t^2 < \infty$  and others,  $\mathbf{w}$  converges to the posterior distribution. The pseudocode of HCM model training are summarized in Algorithm 1 and the PyTorch code is available<sup>1</sup>.

## 2.3 Model Inference for Anomaly Detection

### 2.3.1 Inference

Based on SGLD update, the posterior inference can be achieved by adding Gaussian noise to the gradients at each

1. <https://github.com/Juintin/GraphAnomalyDetection.git>

---

**Algorithm 1** HCM model Training
 

---

**Input:** Initialize a attribute network  $\mathcal{G}$  with nodal attributes  $\mathbf{X}$  and network topology relations  $\mathbf{A}$ , with hyper-parameters drop ratio  $R$ , classes  $C$ , sampling ratio  $S$ , step size  $\epsilon$ ; HCM model  $F_w(\mathbf{X}, \mathbf{A})$ ; the prior distribution of the parameters  $p(\mathbf{w})$ .

**Output:** the trained HCM model  $F_w(\mathbf{X}, \mathbf{A})$

- 1: Drop edges using Eq. 1 or Eq. 2
  - 2: Generate true hop counts  $Y_{hop}$  based on adjacency matrix with dropped edges using Dijkstra search algorithm.
  - 3: Initialize the parameters of HCM model  $\mathbf{w}$
  - 4: **for** each epoch  $i$  **do**
  - 5:    $\hat{Y}_{hop} = F_{w_i}(\mathbf{X}, \mathbf{A})$
  - 6:   Get  $\eta_i \sim \mathcal{N}(0, \epsilon)$
  - 7:    $\delta_{w_i} = \frac{\epsilon}{2}(\nabla_{w_i} \mathcal{L}_{self}(\mathbf{w}_i, \mathbf{A}, \mathbf{X}) + \nabla_{w_i} \log p(\mathbf{w}_i)) + \eta_i$
  - 8:    $\mathbf{w}_{i+1} = \mathbf{w}_i - \delta_{w_i}$
  - 9: **end for**
  - 10: **return**  $F_w(\mathbf{X}, \mathbf{A})$
- 

step and the prediction can be estimated by the posterior sample averages after a "burn in" phase [20]:

$$\tilde{Y}_{hop}(v_i, v_j) = \frac{1}{T} \sum_{t=1}^T F_{w_t}(v_i, v_j | \mathbf{X}, \mathbf{A}) \quad (15)$$

### 2.3.2 Anomaly Scores

Based on HCM model, we design two anomaly criteria for catching anomalies. The first anomaly criterion is the averaged predicted hop counts between a node and its neighbors. Since anomalous nodes are different with their local neighbors, the predicted hop counts are expected to be larger than normal nodes. Therefore, the higher averaged predicted hop counts, the higher probability of being anomalous nodes. The second anomaly criterion combines the averaged predicted hop counts and the inferred variance of posterior samples. [26] showed the evidence that the lack of data could increase the model's uncertainty. Considering that anomalies are rare on the network, the inferred variance on anomalous nodes tends to be higher.

**Average Hop Prediction (AHP)** which is the averaged hop predictions between a node and its neighbors. The expression is defined as followings:

$$S_{AHP}(v_i) = \frac{\sum_{v_j} \tilde{Y}_{hop}(v_i, v_j)}{|\mathcal{N}(v_i)|}, v_j \in \mathcal{N}(v_i), \quad (16)$$

where  $\mathcal{N}(v_i)$  is the neighbors of node  $v_i$ .  $S_{AHP}(v_i)$  represents the averaged hop prediction for node  $v_i$ . For convenience, we use  $S_{AHP}(V)$  denote the averaged hop predictions for all nodes:

$$S_{AHP}(V) = \{S_{AHP}(v_1), S_{AHP}(v_2), \dots, S_{AHP}(v_i)\}, v_i \in V \quad (17)$$

**Average Hop Prediction+Inferred Variance (HAV)** which integrates the averaged hop predictions and inferred variance. The variance of hop prediction between node  $v_i$  and node  $v_j$  is defined as followings:

$$\delta(v_i, v_j) = \frac{\sum_{t=1}^T (F_{w_t}(v_i, v_j | \mathbf{X}, \mathbf{A}) - \tilde{Y}_{hop}(v_i, v_j))^2}{T}, \quad (18)$$

where  $v_i, v_j \in V$ . For one node, we use the averaged variance of hop predictions between the node and its neighbors to present the anomaly scores of this node.

$$S_{IV}(v_i) = \frac{\sum_{v_j} \delta(v_i, v_j)}{|\mathcal{N}(v_i)|}, v_j \in \mathcal{N}(v_i). \quad (19)$$

Similarly, We use  $S_{IV}(V)$  to denote the variance for all nodes.

$$S_{IV}(V) = \{S_{IV}(v_1), S_{IV}(v_2), \dots, S_{IV}(v_i)\}, v_i \in V. \quad (20)$$

Finally, we integrate the anomaly scores from the predicted hop counts and the inferred variance together. The expression is defined as follows:

$$S_{HAV}(V) = \frac{S_{AHP}(V)}{\max(S_{AHP}(V))} + \frac{S_{IV}(V)}{\max(S_{IV}(V))}, \quad (21)$$

where  $\max(\cdot)$  represents the maximum value of the set. Considering that the predicted hop counts and inferred variance have different scales, we use the maximum to normalize each score. The pseudocode of anomaly scores are summarized in Algorithm 2.

---

**Algorithm 2** HCM model Inference for Anomaly Scores
 

---

**Input:** Initialize a attribute network  $\mathcal{G}$  with nodal attributes  $\mathbf{X}$  and network topology relations  $\mathbf{A}$ ; the HCM model  $F_w(\mathbf{X}, \mathbf{A})$ ; the prior distribution of the parameters  $p(\mathbf{w})$ .

**Output:** AHP score  $S_{AHP}(V)$ ; HAV score  $S_{HAV}(V)$

- 1:  $Y \leftarrow \{\}$
  - 2: **for**  $t = 0$  to  $T$  **do**
  - 3:    $\hat{Y}_{hop} = F_{w_t}(\mathbf{X}, \mathbf{A})$
  - 4:    $Y \leftarrow Y + \hat{Y}_{hop}$
  - 5:   Get  $\eta_t \sim \mathcal{N}(0, \epsilon)$
  - 6:    $\delta_{w_t} = \frac{\epsilon}{2}(\nabla_{w_t} \mathcal{L}_{self}(\mathbf{w}_t, \mathbf{A}, \mathbf{X}) + \nabla_{w_t} \log p(\mathbf{w}_t)) + \eta_t$
  - 7:    $\mathbf{w}_{t+1} = \mathbf{w}_t - \delta_{w_t}$
  - 8: **end for**
  - 9: Get  $\tilde{Y}_{hop}$  by averaging  $Y$
  - 10: Get  $\delta$  by calculating the variance of  $Y$
  - 11: Get  $S_{AHP}(V)$  using Eq. 16 and Eq. 17
  - 12: Get  $S_{IV}(V)$  using Eq. 19 and Eq. 20
  - 13: Get  $S_{HAV}(V)$  using Eq. 21
  - 14: **return**  $S_{AHP}(V)$  and  $S_{HAV}(V)$
- 

## 2.4 Complexity Analysis

Our model is composed with tree components. The first component is Preprocess with two operations: Drop Edges and Generating Labels. The complexity of Drop edges is  $O(|E|)$  since it will iterate over all edges. Generating Labels is based on Dijkstra algorithm, so its complexity is  $O((|E| + |V|) \log |V|)$  [27]. The second component is a GCN and its complexity is  $O(|E| \cdot d \cdot \mathbf{F})$  [13], where  $d$  is the dimensions of attributes and  $\mathbf{F}$  is the summation of feature maps among all GCN layers. The third component is MLP, which is composed of fully connected layers. For simplicity, suppose that there are  $s$  training samples,  $t$  input features,  $K$  hidden layers and each has  $h$  neurons, and  $C$  output classes. Its complexity is  $O(s \cdot t \cdot h^k \cdot C)$ . Therefore, the overall complexity is  $O(|E| + (|E| + |V|) \log |V| + (|E| \cdot d \cdot \mathbf{F} + s \cdot t \cdot h^k \cdot C) \cdot i)$  where  $i$  is the number of epochs.

### 3 EXPERIMENTS

In this section, we evaluate our proposed HCM model empirically. We aim to answer the following three research questions:

- RQ1: Is HCM model effective in detecting anomalies on attributed networks?
- RQ2: Does SGLD optimization framework benefit the anomaly detection performance of our approach on attributed networks?
- RQ3: How do the hyper-parameters in HCM model affect the anomaly detection performance?

We first introduce the datasets and experimental settings. Then we report and analyze the experimental results.

#### 3.1 Datasets

We use five real-world attributed networks to evaluate the effectiveness of our proposed method. These networks have been widely used in previous anomaly detection studies [7], [10], [11], [13], [28]. These networks can be categorized into two types: networks with ground-truth anomaly labels and networks with injected anomaly labels.

- For networks with ground-truth anomaly labels, Amazon and Enron<sup>2</sup> have been used. Amazon is a co-purchase network [29]. The anomalous nodes are defined as nodes having the tag *amazonfail*. Enron is an email network [30]. Attributes represent content length, number of recipients, etc, and each edge indicates the email transmission between sender and receiver. Spammers are the anomalies.
- For networks with injected anomaly labels, we select BlogCatalog, Flickr and ACM<sup>3</sup>. BlogCatalog is a blog sharing website. A list of tags associated with each user is used as the attributes. Flickr is an image hosting and sharing website. Similarly, tags are the attributes. ACM is a citation network. Words in abstracts are used as attributes.

A brief statistics of these attributed networks is shown in Table 1. Note that for the data with injected labels, to make a fair comparison, we follow previous studies for anomaly injection [7], [13]. In specific, two anomaly injection methods have been used to inject anomalies by perturbing topological structure and nodal attributes, respectively:

- **Structural anomalies:** we perturb the topological structure of the input network to generate structural anomalies. It is intuitive that small cliques are typically anomalous in which a small set of nodes are much more connected to each other than average [31]. Thus, we inject edges to form small cliques as the structural anomalies following the method used in [7], [13], [32]. In details, we randomly select  $s$  nodes from the network and then make those nodes fully connected, and then all the  $s$  nodes forming the clique are labeled as anomalies.  $t$  cliques are generated repeatedly and totally there are  $s \times t$  structural anomalies.
- **Attribute anomalies:** we perturb the nodal attributes of the input network to generate attribute anomalies. Same to [7], [13], [33], we first randomly select  $s \times t$

nodes as the attribute perturbation candidates. For each selected node  $v_i$ , we randomly select another  $k$  nodes from the network and calculate the Euclidean distance between  $v_i$  and all the  $k$  nodes. Then the node with largest distance is selected as  $v_j$  and the attributes  $\mathbf{X}_j$  of node  $v_j$  is changed to  $\mathbf{X}_i$  of node  $v_i$ . The selected node  $v_j$  is regarded as the generated attribute anomaly.

In the experiments, we set  $s = 15$  and set  $t$  to 10, 15, and 20 for BlogCatalog, Flickr and ACM, respectively which are the same to [7], [13] in order to make a fair comparison. To facilitate the learning process, in our experiments, we use Principal Component Analysis (PCA) [34] to reduce the dimensionality of attributes to 20 following [32].

#### 3.2 Experimental Settings

In the experiments, we use HCM model consisting of four convolution layers and two fully connected layers for Amazon and Enron networks, two convolution layers and two fully connected layers for BlogCatalog, Flickr and ACM networks. The units of each convolution layer is 128. The units of the fully connected layer are set to 256 and the classes  $C$  respectively. The learning rate is set to 0.01. The weight decay is set to  $5e-8$ . The default drop ratio  $R$ , classes  $C$  and sampling ratio  $S$  are set to 0.2, 4 and 0.3 respectively.

#### 3.3 Evaluation Metrics

In the experiments, we use the area under the receiver operating characteristic curve (ROC-AUC) as the evaluation metric for anomaly detection as it has been widely used in previous studies [7], [10], [11], [13], [28]. ROC-AUC can quantify the trade-off between true positive rate (TP) and false positive rate (FP) across different thresholds. The TP is defined as the detection rate, i.e. the rate of true anomalous nodes correctly identified as anomalous, whereas the FP is the false alarm rate, i.e. rate of normal nodes identified as anomalous [28].

#### 3.4 Compared Approaches

We compare the proposed HCM model with the following anomaly detection methods:

- **LOF** [35] measures how isolated the object is with respect to the surrounding neighborhood and detects anomalies at the contextual level. LOF only considers nodal attributes.
- **AMEN** [36] analyzes the abnormality of each node from the ego-network point of view.
- **Radar** [10] detects anomalies by characterizing the residuals of attribute information and its coherence with network information.
- **ANOMALOUS** [11] is a joint anomaly detection framework to select attributes and detect anomalies using CUR decomposition of matrix.
- **DOMINANT** [7] selects anomalies by ranking the reconstruction errors where the errors are learned by GCN.
- **MADAN** [28] uses the heat kernel as filtering operator to exploit the link with the Markov stability to find the context for multi-scale anomalous nodes.

2. <https://www.ipd.kit.edu/mitarbeiter/muellere/consub/>

3. <http://people.tamu.edu/~xhuang/Code.html>

TABLE 1: Statistics of networks.

Dataset	ground-truth anomaly		injected anomaly		
	Amazon	Enron	BlogCatalog	Flickr	ACM
# nodes	1,418	13,533	5,196	7,575	16,484
# edges	3,695	176,987	171,743	239,738	71,980
# attributes	28	20	8,189	12,074	8,337
# anomalies	28	5	300	450	600

- ResGCN [13] learns the residual information using a deep neural network, and reduces the adverse effect from anomalous nodes using the residual-based attention mechanism.

### 3.5 Experimental Results

We conduct experiments to evaluate the performance of our proposed method and to compare it with several state-of-the-art approaches, to which we refer as baselines, on two different types of networks: networks with ground-truth anomalies and injected anomalies respectively.

**Results on the networks with known ground-truth anomalies** Results on the network with ground-truth anomalies are shown in Table 3. It shows that the HCM-HAV score achieves the best among the baselines on Enron network and comparable results on Amazon. The HCM-AHP score leads to comparable results achieved with DOMINANT and ANOMALOUS, which demonstrate the effectiveness of utilizing both global and local information to detect anomalies. The better performance of the HCM-HAV score than the HCM-AHP score indicates that the inferred variance plays a role in finding anomalies in the Amazon and Enron networks.

**Results on the networks with injected anomalies** Results on the network with injected anomalies are shown in table 2. As can be seen, HCM-HAV and HCM-AHP scores outperform the baseline methods in all cases, which further validate the effectiveness of our method by utilizing both global and local information to detect anomalies.

The insight of HCM-AHP is that the hop counts between the anomalous nodes and their neighbors are expected to be larger than that between normal nodes and their neighbors, and the insight of HCM-HAV score integrates the influence of inferred variance into HCM-AHP. Fig. 3 shows that the average HCM-AHP and HCM-HAV among anomalous nodes are bigger than among non-anomalous nodes, which further validates the rationality of the insight. Interestingly, we note that the HCM-HAV score doesn’t perform better than HCM-AHP score on BlogCatalog and ACM networks, which indicates that the integration of inferred variance and HCM-AHP score does not always improve the performance. However, HCM-HAV can consistently achieve good results on all networks compared to HCM-AHP.

### 3.6 Ablation Study

For our proposed HCM model, SGLD is used instead of stochastic gradient descent (SGD) to optimize the model since we adopt Bayesian learning. Here we conduct experiments to show the benefits of utilizing SGLD to train our proposed model. Specifically, we firstly test the anomaly detection performances of model optimized by SGD and

TABLE 2: Performance of different anomaly detection methods w.r.t. ROC-AUC on Flickr, BlogCatalog and ACM networks.

	Flickr	BlogCatalog	ACM
LOF [35]	0.488	0.491	0.473
AMEN [36]	0.604	0.665	0.533
Radar [10]	0.728	0.725	0.693
ANOMALOUS [11]	0.716	0.728	0.718
DOMINANT [7]	0.781	0.749	0.749
SCAN [28]	0.268	0.273	0.359
ResGCN [13]	0.780	0.785	0.768
HCM-AHP (Ours)	0.791	<b>0.808</b>	<b>0.806</b>
HCM-HAV (Ours)	<b>0.792</b>	0.798	0.761

TABLE 3: Performance of different anomaly detection methods w.r.t. ROC-AUC on Amazon and Enron networks.

	Amazon	Enron
LOF [35]	0.490	0.440
AMEN [36]	0.470	0.470
Radar [10]	0.580	0.650
ANOMALOUS [11]	0.602	0.695
DOMINANT [7]	0.625	0.685
MADAN [28]	0.680	0.680
ResGCN [13]	<b>0.710</b>	0.660
HCM-AHP (Ours)	0.62	0.670
HCM-HAV (Ours)	0.708	<b>0.715</b>

SGLD respectively. Then we monitor the trend of ROC-AUC during the training process under SGD and SGLD training strategy respectively. The results are shown in Fig. 4, Fig. 5 and Fig. 6. We can observe the following from these figures:

- From Fig. 4 and Fig. 5, we see that the ROC-AUC performance achieved by SGLD is better than that by SGD on Flickr and ACM networks, which shows that SGLD based Bayesian learning benefits the anomaly detection on attributed networks.
- From Fig. 6, we can see that the AUC trend under SGLD is steadier than that under SGD.

### 3.7 Parameter Analysis

We conducted a series of experiments to study the impact of hyper-parameters on the performance of anomaly detection. There are three hyper-parameters introduced in our proposed methods: (1) drop ratio  $R$  in the Preprocess component, which controls the percentages of dropped edges, (2) classes  $C$ , that controls the max hop counts that training set contains, (3) sampling ratio  $S$ , that controls the amount of node pairs engaging in the training process of each iteration.

**Drop Ratio  $R$ .** We fix classes  $C$  and sampling ratio  $S$  to 5 and 0.3 respectively. Then we monitor the anomaly performance by ranging drop ratio  $R$  from 0 to 0.5 on BlogCatalog, Flickr and ACM networks. The results are showed in Fig. 7.

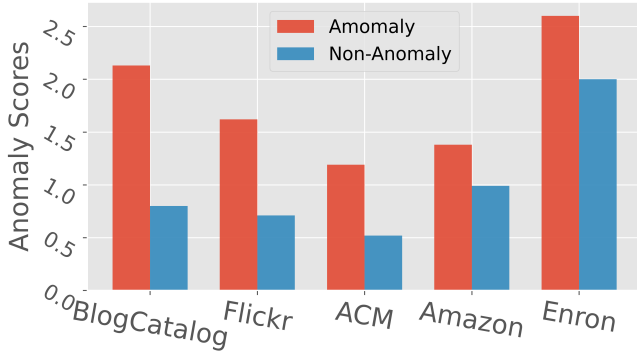
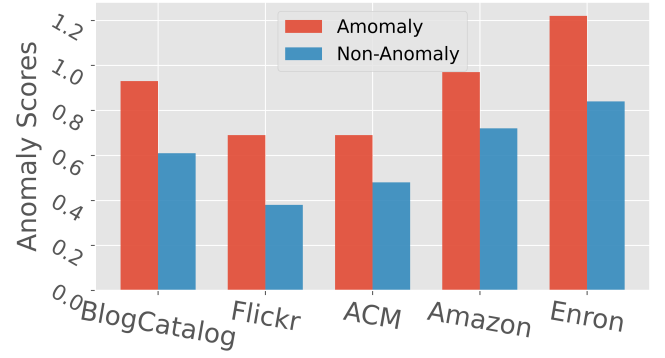
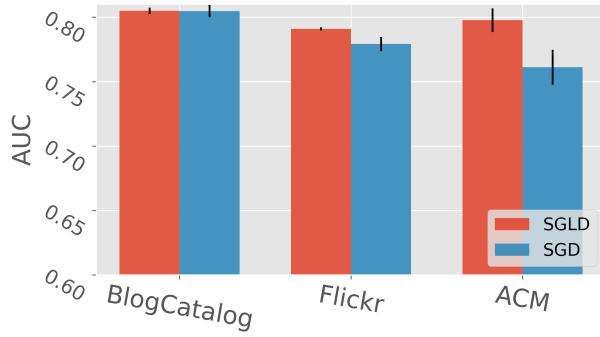
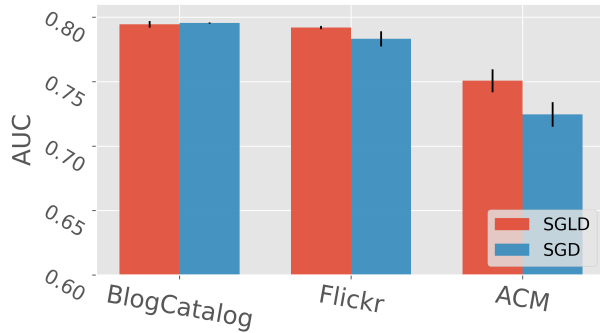
(a) Average  $S_{AHP}$ (b) Average  $S_{HAV}$ 

Fig. 3: Average Scores of Anomalous nodes and Non-Anomalous nodes

Fig. 4: ROC-AUC achieved by  $S_{AHP}$  under SGLD and SGD training strategy respectively.Fig. 5: ROC-AUC achieved by  $S_{HAV}$  under SGLD and SGD training strategy respectively.

From Fig. 7 we can see that removing a few edges with low similarity is beneficial to detect anomalies. Specifically, the experiments show that the performance of anomaly detection increases greatly on BlogCatalog and Flickr networks when a few edges are removed. However, it is not encouraged to remove a large amount of edges since the performance of anomaly detection has slightly decreased when a large amount of edges are removed.

**Classes  $C$ .** We set drop ratio  $R$  and sampling ratio  $S$  to 0.2 and 0.3 respectively. The classes  $C$  varies from 2 to 7. Experiments are made on BlogCatalog, Flickr and ACM

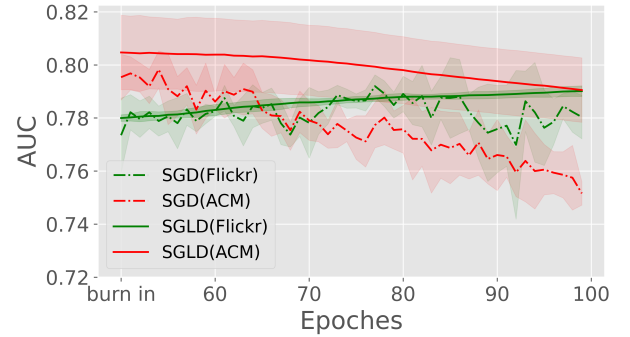


Fig. 6: ROC-AUC trends during the training process under SGLD and SGD training strategy respectively. The ROC-AUC value is the mean of 10 times repeated experiments. The filled region along trends is the standard deviation of the 10 times repeated experiments.

networks and the results are showed in Fig. 8.

From Fig. 8, we can see that the performance of anomaly detection is improved with the increase of the classes  $C$ , especially on Flickr and BlogCatalog networks. The improvement suggests that the global information are beneficial to the anomaly detection since the more classes  $C$ , the more global information are used.

**Sampling Ratio  $S$ .** We fix hyper-parameters  $R$  and  $C$  to 0.2 and 5 respectively. The we set sampling ratio  $S$  varying from 0.1 to 1.0. Experiments are made on BlogCatalog, Flickr and ACM networks. The results are showed in Fig. 9.

From Fig. 9, we can see that the performance of detecting anomaly is insensitive to sampling ratio  $S$ .

### 3.8 Summary

To summarise, our experimental evaluation provides conclusive answers to the three three main questions formulated at the start of Section 3. For RQ1, the superior performance of detecting anomalous nodes (Table 3 and Table 2) on five real-world networks shows the evidence that our approach can effectively detect anomalies on attributed networks. Besides, the significant difference of  $S_{AHP}$  and  $S_{HAV}$  scores between anomalous nodes and

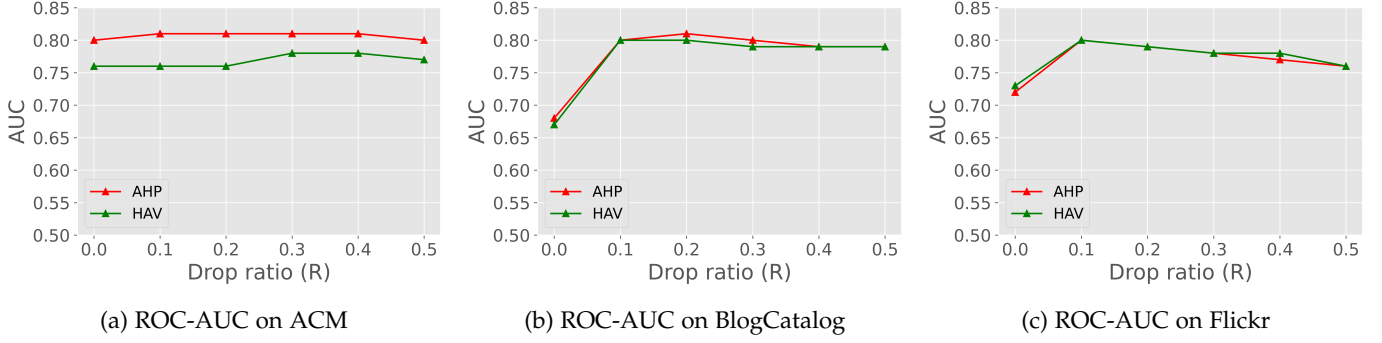


Fig. 7: Influence of the hyper-parameter: drop ratio ( $R$ ) (ranging from 0.0 to 0.5): (a) ROC-AUC on ACM, (b) ROC-AUC on BlogCatalog, and (c) ROC-AUC on Flickr.

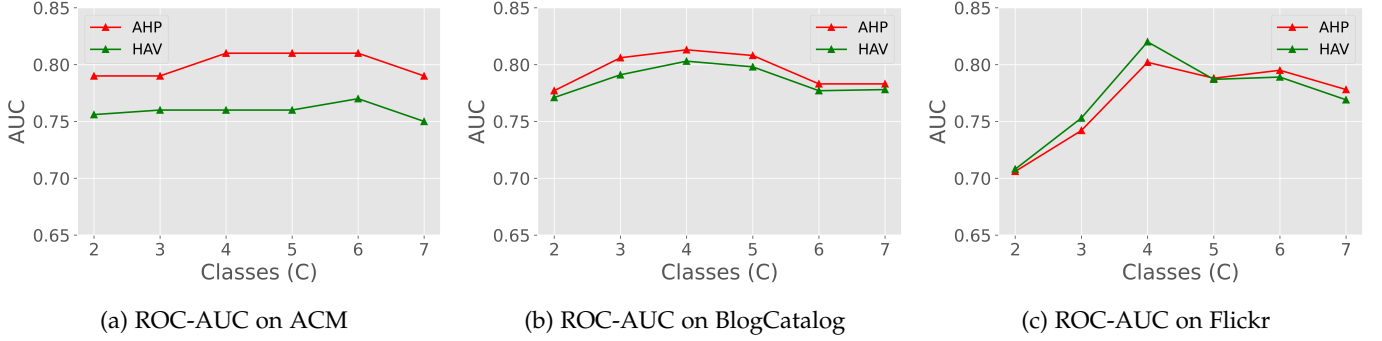


Fig. 8: Influence of the hyper-parameter: classes ( $C$ ) (ranging from 2 to 7): (a) ROC-AUC on ACM, (b) ROC-AUC on BlogCatalog, and (c) ROC-AUC on Flickr.

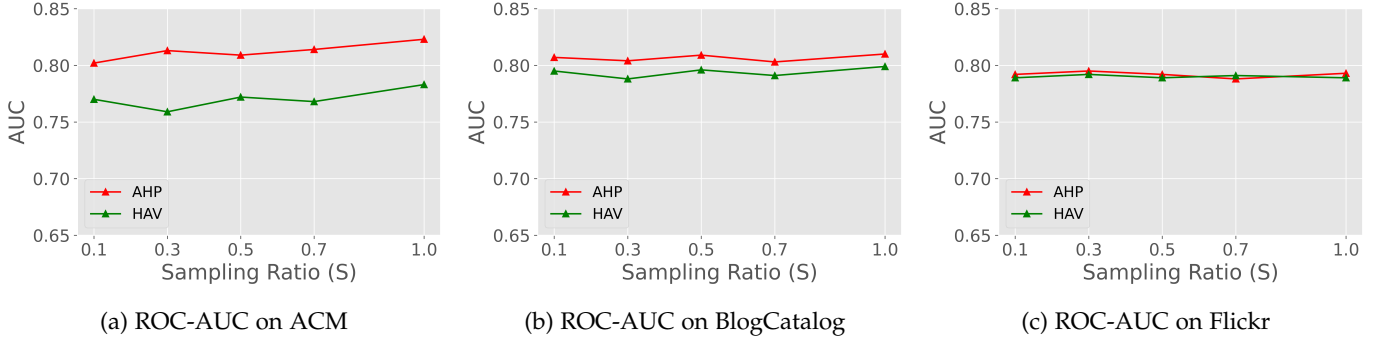


Fig. 9: Influence of the hyper-parameter: Sampling Ratio ( $S$ ) (ranging from 0.1 to 1.0): (a) ROC-AUC on ACM, (b) ROC-AUC on BlogCatalog, and (c) ROC-AUC on Flickr.

non-anomalous nodes further (Fig. 3) indicates that hop count is an informative indicator of anomalies. For RQ2, the better performance w.r.t ROC-AUC of SGLD based training strategy than SGD based training strategy (Fig. 4, Fig. 5 and Fig. 6) shows the evidence that SGLD based Bayesian framework can further improve the performance of our method in detecting anomalies on attributed networks. For RQ3, the parameter analysis shows that a small value of  $R$  and a moderate value of  $C$  can improve the performance of our approach in detecting anomalies on attributed network but large value of  $R$  and  $C$  could lead to a negative effect (Fig. 7 and Fig. 8). Besides, the parameter analysis also show that our approach is not sensitive to the randomly sampling ratio  $S$  (Fig. 9).

## 4 RELATED WORK

In this section, we provide a more elaborate overview of related work on anomaly detection on graphs and self-supervised learning.

### 4.1 Anomaly Detection on Graphs

Anomaly detection is one of the most important research questions in different types of data, e.g., text [37], [38], network [39], time series [40] and temporal data [41]. Compared to anomaly detection approaches on other types of data, anomaly detection on attributed networks is more challenging because both structures and attributes should be taken into consideration. Different approaches from dif-

ferent aspects have been proposed to detect anomalies on attributed graphs in the literature.

CODA [8] focuses on community anomalies by simultaneously finding communities as well as spotting anomalies using a unified probabilistic model. AMEN [36] uses both attribute and network structure information to detect anomalous neighborhoods. Radar [10] detects anomalies whose behaviors are singularly different from the majority by characterizing the residuals of attribute information and its coherence with network information. ANOMALOUS [11] is a joint anomaly detection framework to optimize attribute selection and anomaly detection using CUR decomposition of matrix and residual analysis on attributed networks. MADAN [28] is a multi-scale anomaly detection method. It uses the heat kernel as filtering operator to exploit the link with the Markov stability to find the context for outlier nodes at all relevant scales of the network.

With the popularity of network embedding techniques, which assigns nodes in a network to low-dimensional representations and these representations can effectively preserve the network structure [42], learning anomaly aware network representations also attracts huge attentions. Recently, there are several studies taking both problems into consideration to learn anomaly aware network embedding in attributed networks [7], [12], [13], [43]. SEANO [12] is a semi-supervised network embedding approach which learns a low-dimensional vector representation that systematically captures the topological proximity, attribute affinity and label similarity of nodes. ONE [43] jointly align and optimize the structures and attributes to generate robust network embeddings by minimizing the effects of outlier nodes. DOMINANT [7] utilizes GCN learn low-dimensional embedding representations and then reconstruct both the topological structure and nodal attributes with these representations. ResGCN [13] combines GCN and residual modeling to detect anomalies based on learned residual information.

## 4.2 Self-supervised Learning

Self-supervised learning is used to learn features from unlabeled data and mitigate the time-consuming problem of labeling large-scale data. It has been shown that self-supervised learning substantially improves accuracy on semi-supervised tasks [44]. Besides, self-supervised learning also improves model’s robustness and uncertainty estimation, including robustness to adversarial examples, label corruption, common input corruption and benefiting out-of-distribution detection on difficulty, near-distribution outliers [14]. A technical definition of self-supervised learning is that it refers to learning methods where they automatically generate supervisory signals to train a model by constructing some self-supervised tasks (also known as proxy tasks) according to the data alone. The self-supervised tasks usually share two properties [45]: (1) The features learned by the model can be used to solve the self-supervised tasks; (2) The labels of the self-supervised tasks can be automatically generated according to the data only.

Recently, a wide variety of self-supervised learning methods have been proposed on computer vision, each exploring a different of self-supervised task. According to

the type of self-supervised task, self-supervised learning can be categorized into four categories [45]. The first is Generation-based methods: This type of methods learn features via solving self-supervised tasks that related to image or video generation, e.g. image colorization [46], image inpainting [47], image super resolution [48], video prediction [49] and etc. The second is Context-based pretext tasks: This type of methods employ the context features of images or videos, e.g. Context similarity based methods [50], [51], Spatial context structure based methods [52], [53], [54], Temporal context structure based on methods [55], [56] and etc. The third is Free semantic label-based Methods: This type of methods utilize traditional algorithms to generate labels for constructing the self-supervised task, e.g. contour detection [57], moving object segmentation [58], relative depth prediction [59] and etc. The fourth is Cross Modal-based Methods: This type of methods utilize different channels of images to construct supervisory signals, e.g. RGB-Flow correspondence verification [60], egomotion [61] and etc.

Most recently, self-supervised learning techniques are explored in graph convolutional networks (GCNs). [21] explores the effect of applying three self-supervised tasks in GCNs and demonstrate that a properly designed self-supervised task can improve the generalizability and robustness of GCNs. [15] utilizes self-supervised tasks to learn representation that can catch the global structure of the graph, which is shown to be beneficial to downstream tasks. [22] explores the impact of more self-supervised tasks in graph neural networks (GNNs).

## 5 CONCLUSION

In this paper, we proposed HCM model based on self-supervised technique for anomaly detection. To the best of our knowledge, it is the first model to take both local and global contextual information into account for anomaly detection. Specifically, we utilize a hop-count based self-supervised task to learn node representation with capturing local and global contextual information. The learned node representation will be used to predict hop counts for arbitrary node pairs as well. Besides, we design two new anomaly scores for detecting anomalies based on the hop counts prediction via HCM model. Finally, we introduce SGLD to train the model for capturing uncertainty in learned parameters and avoid overfitting. The extensive experiments demonstrate: 1) the consistent effectiveness of the HCM model in anomaly detection on attributed networks that we proposed; 2) SGLD-based Bayesian learning strategy is beneficial to achieve a better and stable performance in detecting anomalies.

## ACKNOWLEDGMENTS

This research is partly supported by NWO. Tianjin Huang is supported by the China Scholarship Council.

## REFERENCES

- [1] Y. Pei, N. Chakraborty, and K. Sycara, “Nonnegative matrix tri-factorization with graph regularization for community detection in social networks,” in *Twenty-Fourth International Joint Conference on Artificial Intelligence*, 2015.

- [2] I. Falih, N. Grozavu, R. Kanawati, and Y. Bennani, "Community detection in attributed network," in *Companion Proceedings of the The Web Conference 2018*, 2018, pp. 1299–1306.
- [3] J. Li, K. Cheng, L. Wu, and H. Liu, "Streaming link prediction on dynamic attributed networks," in *Proceedings of the Eleventh ACM International Conference on Web Search and Data Mining*, 2018, pp. 369–377.
- [4] R. Brochier, A. Guille, and J. Velcin, "Link prediction with mutual attention for text-attributed networks," in *Companion Proceedings of The 2019 World Wide Web Conference*, 2019, pp. 283–284.
- [5] X. Huang, J. Li, and X. Hu, "Accelerated attributed network embedding," in *Proceedings of the 2017 SIAM international conference on data mining*. SIAM, 2017, pp. 633–641.
- [6] Z. Meng, S. Liang, H. Bao, and X. Zhang, "Co-embedding attributed networks," in *Proceedings of the Twelfth ACM International Conference on Web Search and Data Mining*, 2019, pp. 393–401.
- [7] K. Ding, J. Li, R. Bhanushali, and H. Liu, "Deep anomaly detection on attributed networks," in *Proceedings of the 2019 SIAM International Conference on Data Mining*. SIAM, 2019, pp. 594–602.
- [8] J. Gao, F. Liang, W. Fan, C. Wang, Y. Sun, and J. Han, "On community outliers and their efficient detection in information networks," in *Proceedings of the 16th ACM SIGKDD international conference on Knowledge discovery and data mining*, 2010, pp. 813–822.
- [9] B. Perozzi, L. Akoglu, P. Iglesias Sánchez, and E. Müller, "Focused clustering and outlier detection in large attributed graphs," in *Proceedings of the 20th ACM SIGKDD international conference on Knowledge discovery and data mining*, 2014, pp. 1346–1355.
- [10] J. Li, H. Dani, X. Hu, and H. Liu, "Radar: Residual analysis for anomaly detection in attributed networks." in *IJCAI*, 2017, pp. 2152–2158.
- [11] Z. Peng, M. Luo, J. Li, H. Liu, and Q. Zheng, "Anomalous: A joint modeling approach for anomaly detection on attributed networks." in *IJCAI*, 2018, pp. 3513–3519.
- [12] J. Liang, P. Jacobs, J. Sun, and S. Parthasarathy, "Semi-supervised embedding in attributed networks with outliers," in *Proceedings of the 2018 SIAM International Conference on Data Mining*. SIAM, 2018, pp. 153–161.
- [13] Y. Pei, T. Huang, W. van Ipenburg, and M. Pechenizkiy, "Resgcn: Attention-based deep residual modeling for anomaly detection on attributed networks," *arXiv preprint arXiv:2009.14738*, 2020.
- [14] D. Hendrycks, M. Mazeika, S. Kadavath, and D. Song, "Using self-supervised learning can improve model robustness and uncertainty," in *Advances in Neural Information Processing Systems*, 2019, pp. 15 663–15 674.
- [15] Z. Peng, Y. Dong, M. Luo, X.-M. Wu, and Q. Zheng, "Self-supervised graph representation learning via global context prediction," *arXiv preprint arXiv:2003.01604*, 2020.
- [16] S. Cao, W. Lu, and Q. Xu, "Grarep: Learning graph representations with global structural information," in *Proceedings of the 24th ACM international on conference on information and knowledge management*, 2015, pp. 891–900.
- [17] Y. Pei, X. Du, J. Zhang, G. Fletcher, and M. Pechenizkiy, "struc2gauss: Structural role preserving network embedding via gaussian embedding," *DATA MINING AND KNOWLEDGE DISCOVERY*, 2020.
- [18] R. A. Rossi, N. K. Ahmed, and E. Koh, "Higher-order network representation learning," in *Companion Proceedings of the The Web Conference 2018*, 2018, pp. 3–4.
- [19] Y. Pei, *On local and global graph structure mining*, ser. SIKS Dissertation Series. Technische Universiteit Eindhoven, 2020, no. 2020-05.
- [20] M. Welling and Y. W. Teh, "Bayesian learning via stochastic gradient langevin dynamics," in *Proceedings of the 28th international conference on machine learning (ICML-11)*, 2011, pp. 681–688.
- [21] Y. You, T. Chen, Z. Wang, and Y. Shen, "When does self-supervision help graph convolutional networks?" *arXiv preprint arXiv:2006.09136*, 2020.
- [22] W. Jin, T. Derr, H. Liu, Y. Wang, S. Wang, Z. Liu, and J. Tang, "Self-supervised learning on graphs: Deep insights and new direction," *arXiv preprint arXiv:2006.10141*, 2020.
- [23] H. Wu, C. Wang, Y. Tyshetskiy, A. Docherty, K. Lu, and L. Zhu, "Adversarial examples for graph data: deep insights into attack and defense," in *Proceedings of the 28th International Joint Conference on Artificial Intelligence*. AAAI Press, 2019, pp. 4816–4823.
- [24] T. N. Kipf and M. Welling, "Semi-supervised classification with graph convolutional networks," *arXiv preprint arXiv:1609.02907*, 2016.
- [25] W. Hamilton, Z. Ying, and J. Leskovec, "Inductive representation learning on large graphs," in *Advances in Neural Information Processing Systems*, 2017, pp. 1024–1034.
- [26] A. Kendall and Y. Gal, "What uncertainties do we need in bayesian deep learning for computer vision?" in *Advances in neural information processing systems*, 2017, pp. 5574–5584.
- [27] D. B. Johnson, "Efficient algorithms for shortest paths in sparse networks," *Journal of the ACM (JACM)*, vol. 24, no. 1, pp. 1–13, 1977.
- [28] L. Gutiérrez-Gómez, A. Bovet, and J.-C. Delvenne, "Multi-scale anomaly detection on attributed networks," *arXiv preprint arXiv:1912.04144*, 2019.
- [29] E. Müller, P. I. Sánchez, Y. Mülle, and K. Böhm, "Ranking outlier nodes in subspaces of attributed graphs," in *2013 IEEE 29th International Conference on Data Engineering Workshops (ICDEW)*. IEEE, 2013, pp. 216–222.
- [30] V. Metsis, I. Androutsopoulos, and G. Paliouras, "Spam filtering with naive bayes-which naive bayes?" in *CEAS*, vol. 17. Mountain View, CA, 2006, pp. 28–69.
- [31] D. B. Skillicorn, "Detecting anomalies in graphs," in *2007 IEEE Intelligence and Security Informatics*. IEEE, 2007, pp. 209–216.
- [32] K. Ding, J. Li, and H. Liu, "Interactive anomaly detection on attributed networks," in *Proceedings of the Twelfth ACM International Conference on Web Search and Data Mining*, 2019, pp. 357–365.
- [33] X. Song, M. Wu, C. Jermaine, and S. Ranka, "Conditional anomaly detection," *IEEE Transactions on knowledge and Data Engineering*, vol. 19, no. 5, pp. 631–645, 2007.
- [34] S. Wold, K. Esbensen, and P. Geladi, "Principal component analysis," *Chemometrics and intelligent laboratory systems*, vol. 2, no. 1-3, pp. 37–52, 1987.
- [35] M. M. Breunig, H.-P. Kriegel, R. T. Ng, and J. Sander, "Lof: identifying density-based local outliers," in *Proceedings of the 2000 ACM SIGMOD international conference on Management of data*, 2000, pp. 93–104.
- [36] B. Perozzi and L. Akoglu, "Scalable anomaly ranking of attributed neighborhoods," in *Proceedings of the 2016 SIAM International Conference on Data Mining*. SIAM, 2016, pp. 207–215.
- [37] R. Kannan, H. Woo, C. C. Aggarwal, and H. Park, "Outlier detection for text data," in *Proceedings of the 2017 siam international conference on data mining*. SIAM, 2017, pp. 489–497.
- [38] L. Ruff, Y. Zemlyanskiy, R. Vandermeulen, T. Schnake, and M. Kloft, "Self-attentive, multi-context one-class classification for unsupervised anomaly detection on text," in *Proceedings of the 57th Annual Meeting of the Association for Computational Linguistics*, 2019, pp. 4061–4071.
- [39] M. H. Bhuyan, D. K. Bhattacharyya, and J. K. Kalita, "Network anomaly detection: methods, systems and tools," *Ieee communications surveys & tutorials*, vol. 16, no. 1, pp. 303–336, 2013.
- [40] P. Malhotra, L. Vig, G. Shroff, and P. Agarwal, "Long short term memory networks for anomaly detection in time series," in *Proceedings*, vol. 89. Presses universitaires de Louvain, 2015, pp. 89–94.
- [41] M. Gupta, J. Gao, C. C. Aggarwal, and J. Han, "Outlier detection for temporal data: A survey," *IEEE Transactions on Knowledge and Data Engineering*, vol. 26, no. 9, pp. 2250–2267, 2013.
- [42] P. Cui, X. Wang, J. Pei, and W. Zhu, "A survey on network embedding," *IEEE Transactions on Knowledge and Data Engineering*, vol. 31, no. 5, pp. 833–852, 2018.
- [43] S. Bandyopadhyay, N. Lokesh, and M. N. Murty, "Outlier aware network embedding for attributed networks," in *Proceedings of the AAAI Conference on Artificial Intelligence*, vol. 33, 2019, pp. 12–19.
- [44] X. Zhai, A. Oliver, A. Kolesnikov, and L. Beyer, "S4l: Self-supervised semi-supervised learning," in *Proceedings of the IEEE international conference on computer vision*, 2019, pp. 1476–1485.
- [45] L. Jing and Y. Tian, "Self-supervised visual feature learning with deep neural networks: A survey," *IEEE Transactions on Pattern Analysis and Machine Intelligence*, 2020.
- [46] R. Zhang, P. Isola, and A. A. Efros, "Colorful image colorization," in *European conference on computer vision*. Springer, 2016, pp. 649–666.
- [47] D. Pathak, P. Krahenbuhl, J. Donahue, T. Darrell, and A. A. Efros, "Context encoders: Feature learning by inpainting," in *Proceedings of the IEEE conference on computer vision and pattern recognition*, 2016, pp. 2536–2544.
- [48] C. Ledig, L. Theis, F. Huszár, J. Caballero, A. Cunningham, A. Acosta, A. Aitken, A. Tejani, J. Totz, Z. Wang et al., "Photo-realistic single image super-resolution using a generative adver-

- sarial network," in *Proceedings of the IEEE conference on computer vision and pattern recognition*, 2017, pp. 4681–4690.
- [49] N. Srivastava, E. Mansimov, and R. Salakhudinov, "Unsupervised learning of video representations using lstms," in *International conference on machine learning*, 2015, pp. 843–852.
- [50] M. Caron, P. Bojanowski, A. Joulin, and M. Douze, "Deep clustering for unsupervised learning of visual features," in *Proceedings of the European Conference on Computer Vision (ECCV)*, 2018, pp. 132–149.
- [51] M. Noroozi, A. Vinjimoor, P. Favaro, and H. Pirsiavash, "Boosting self-supervised learning via knowledge transfer," in *Proceedings of the IEEE Conference on Computer Vision and Pattern Recognition*, 2018, pp. 9359–9367.
- [52] L. Jing and Y. Tian, "Self-supervised spatiotemporal feature learning by video geometric transformations," *arXiv preprint arXiv:1811.11387*, vol. 2, no. 7, p. 8, 2018.
- [53] C. Wei, L. Xie, X. Ren, Y. Xia, C. Su, J. Liu, Q. Tian, and A. L. Yuille, "Iterative reorganization with weak spatial constraints: Solving arbitrary jigsaw puzzles for unsupervised representation learning," in *Proceedings of the IEEE Conference on Computer Vision and Pattern Recognition*, 2019, pp. 1910–1919.
- [54] C. Doersch, A. Gupta, and A. A. Efros, "Unsupervised visual representation learning by context prediction," in *Proceedings of the IEEE international conference on computer vision*, 2015, pp. 1422–1430.
- [55] H.-Y. Lee, J.-B. Huang, M. Singh, and M.-H. Yang, "Unsupervised representation learning by sorting sequences," in *Proceedings of the IEEE International Conference on Computer Vision*, 2017, pp. 667–676.
- [56] I. Misra, C. L. Zitnick, and M. Hebert, "Shuffle and learn: unsupervised learning using temporal order verification," in *European Conference on Computer Vision*. Springer, 2016, pp. 527–544.
- [57] I. Croitoru, S.-V. Bogolin, and M. Leordeanu, "Unsupervised learning from video to detect foreground objects in single images," in *Proceedings of the IEEE International Conference on Computer Vision*, 2017, pp. 4335–4343.
- [58] H. Jiang, G. Larsson, M. Maire Greg Shakhnarovich, and E. Learned-Miller, "Self-supervised relative depth learning for urban scene understanding," in *Proceedings of the European Conference on Computer Vision (ECCV)*, 2018, pp. 19–35.
- [59] Y. Li, M. Paluri, J. M. Rehg, and P. Dollár, "Unsupervised learning of edges," in *Proceedings of the IEEE Conference on Computer Vision and Pattern Recognition*, 2016, pp. 1619–1627.
- [60] N. Sayed, B. Brattoli, and B. Ommer, "Cross and learn: Cross-modal self-supervision," in *German Conference on Pattern Recognition*. Springer, 2018, pp. 228–243.
- [61] P. Agrawal, J. Carreira, and J. Malik, "Learning to see by moving," in *Proceedings of the IEEE international conference on computer vision*, 2015, pp. 37–45.